

Ring–chain tautomerism and protolytic equilibria of 3-hydroxy-3-phosphonoisobenzofuranone studied by ^1H , ^{13}C and ^{31}P NMR-controlled titrations^{†‡}

Sven Augner,^a Jan Kehler,^b Zoltán Szakács,^{ac} Eli Breuer^{*b} and Gerhard Hägele^{*a}

Received (in Montpellier, France) 9th January 2008, Accepted 29th April 2008

First published as an Advance Article on the web 30th June 2008

DOI: 10.1039/b800450c

Treatment of 3-chloro-3-(dimethylphosphono)isobenzofuranone (**3**) with NaI in acetonitrile caused its monodemethylation to sodium 3-chloro-3-(methylphosphonato)isobenzofuranone (**4**). Compound **4** hydrolyzed in aqueous solution slowly to 3-hydroxy-3-(methylphosphono)isobenzofuranone (**5**). Upon refluxing in water, **4** demethylated simultaneously with the hydrolysis of the chloride, to afford 3-hydroxy-3-phosphonoisobenzofuranone (**6**). NMR spectra of the 3-hydroxyphosphonoisobenzofuranone derivatives **5** and **6** were found to be pH dependent. Raising the pH of the aqueous solutions to 10 by adding Na_2CO_3 caused changes in their ^{13}C and ^{31}P spectra, indicating opening of the isobenzofuranone ring and the formation of *ortho*-phosphonatoformylbenzoate anions (**7**) and (**8**). Acidification of solutions of **7** and **8** yielded **5** and **6**, via *ortho*-phosphonoformylbenzoic acids (**9**) and (**10**), respectively, as putative intermediates. The facile formation of the cyclic tautomers **3**, **4**, **5** and **6**, is interpreted in terms of the strong electron withdrawing effect of the phosphonyl group. High-resolution 1D and 2D NMR spectra observing nuclei ^1H , ^{13}C and ^{31}P established the molecular structures. Macroscopic dissociation constants were determined for a triprotic acid of type H_3L . Using sensor nuclei ^1H , ^{13}C and ^{31}P in advanced techniques of NMR controlled titrations confirmed concerted protolytic and ring–chain tautomeric equilibria. Probabilities of different sequences of protonation are discussed.

Introduction

Anions of various bisphosphonic¹ (BP) and phosphonocarboxylic acids² have been shown to interact with Ca^{2+} and to inhibit scale formation. In addition, both phosphonocarboxylates and bisphosphonates have been shown to possess biological activity in pathological conditions that involve irregularities in calcium metabolism: such as some bone related diseases that are characterized by excessive destruction of the bone by resorption,³ or conditions that involve ectopic calcification characterized by the pathological deposition of calcium phosphate in a number of clinically important

diseases.⁴ The antiviral pyrophosphate analogs, phosphonoacetic and phosphonoformic acids have also been reported to accumulate in bone and teeth which detracts from their value as drugs.⁵

In another approach, it was reported in previous papers from our laboratory that bisacylphosphonates⁶ and to a lesser extent, other long-chain bisphosphonates⁷ are also biologically active in calcium related disorders. X-Ray crystallographic results indicate that bisacylphosphonates interact with calcium ions to form polynuclear structures in which each terminus of the molecule is bound to a separate calcium ion, which is bound to additional bisacylphosphonates.⁸ This is in contrast to geminal BPs which are pictured as binding calcium ions as bi- or tridentate chelates.¹ Since the bisphosphonates, phosphonocarboxylates and bisacylphosphonates examined so far are all conformationally flexible open chain compounds, we considered it of interest to examine other types of structures which can be expected to interact with hydroxyapatite (HAP), and more generally with calcium, and yield new biologically active compounds. Thus, we were interested to synthesize and to examine compounds in which an acylphosphonic function would be in the proximity of a carboxy function in a conformationally constrained manner, where the two acidic groups would be situated favorably for a chelate formation. For the first target compound fulfilling these structural requirements we had chosen *ortho*-phosphonoformylbenzoic acid (**10**). A search in the literature revealed the existence of 3-chloro-3-(dimethylphosphono)isobenzofuranone (**3**)⁹ which

^a *Inorganic Chemistry and Structural Chemistry, Heinrich-Heine-University Düsseldorf, Universitätsstrasse 1, D-40225 Düsseldorf, Germany. E-mail: haegele@uni-duesseldorf.de; Fax: +49-211-81-11854; Tel: +49-211-81-13166*

^b *Department of Medicinal Chemistry and Natural Products, School of Pharmacy, The Hebrew University of Jerusalem, P.O.B. 12065, Jerusalem, 91120, Israel. E-mail: eli.breuer@huji.ac.il; Fax: +972-2-675-8934; Tel: +972-2-675-8704*

^c *Laboratory for Speciation, Drug and Trace Analysis, Institute of Chemistry, Eötvös Loránd University, Pázmány Péter sétány 1/A, H-1117 Budapest, Hungary. E-mail: szakacs@chem.elte.hu*

[†] (a) Partial preliminary account of this work was presented by J. Kehler and E. Breuer as poster #P28 at the 14th International Conference on Phosphorus Chemistry in July 1998, in Cincinnati, OH, USA, (b) part of a lecture “NMR controlled Titrations”, given by G. Hägele at the ANZMAG conference 2002, Taupo, New Zealand (Australian and New Zealand Society for Magnetic Resonance).

[‡] Electronic supplementary information (ESI) available: Tables S1–S3 and Fig. S1–S12. See DOI: 10.1039/b800450c

we considered a suitable starting material for our target compound. This paper reports the results from our studies regarding the hydrolysis of 3-chloro-3-(dimethylphosphono)isobenzofuranone (**3**) to 3-hydroxy-3-phosphonoisobenzofuranone (**6**),§ which is the cyclic tautomer of *ortho*-(phosphonoformyl)benzoic acid (**10**) and hence the phospho analog of phthalonic acid.

Being aware of the phenomenon of ring-chain tautomerism shown by 3-hydroxy-3-alkyl or aryl isobenzofuranone derivatives that are in equilibrium with the corresponding 2-acylbenzoic acids,¹⁰ we anticipated the possibility of such a tautomeric equilibrium in this case, as well. Indeed, extended analytical and NMR studies of **6** enabled the observation of concerted protolytic and ring-chain tautomeric equilibria.

Practically all previous relevant studies on the ring-chain tautomerism of structurally related compounds had used the isobenzofuranone-*ortho*-acylbenzoate nomenclature. For comparison we will retain this notation even when 3-hydroxy-3-phosphonoisobenzofuranone (**6**) should be named 1,3-dihydro-1-hydroxy-3-oxoisobenzofurane-1-phosphonic acid, following the standard IUPAC nomenclature rules.

Results and discussion

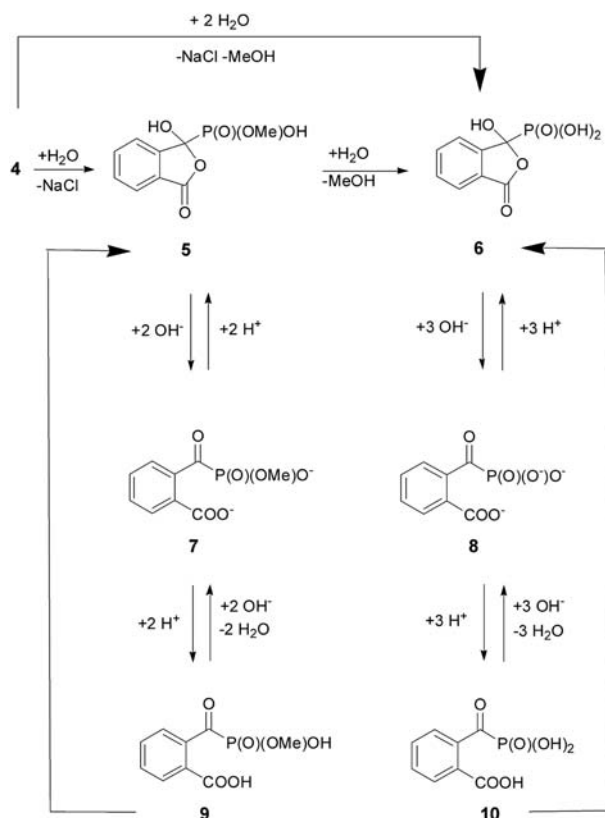
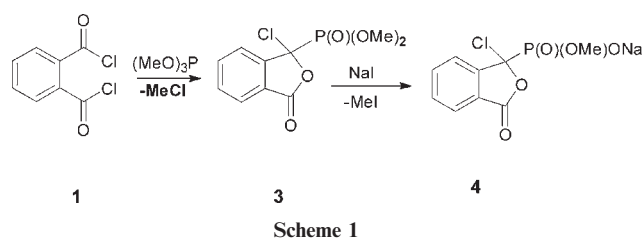
Syntheses

Arbuzov reaction of phthaloyl chloride (**1**) with trimethyl phosphite (**2**) (see Scheme 1) gave 3-chloro-3-(dimethylphosphono)isobenzofuranone (**3**) in good yield.¹¹

Compound **3** could be monodemethylated smoothly to **4** by treatment with sodium iodide in acetonitrile at room temperature. As expected, the tertiary chloride was not displaced by this typical S_N2 reagent. The sodium phosphonate **4** showed a quartet in the proton-coupled ³¹P NMR spectrum at 7.0 ppm, consistent with one POME group. Monitoring an aqueous solution of **4** kept at room temperature showed that it slowly hydrolyzed to a product having a phosphorus signal at 10 ppm which was identified as 3-hydroxy-3-(methylphosphono)isobenzofuranone (**5**). In contrast, refluxing an aqueous solution of **4** caused demethylation of the phosphonic acid ester simultaneously with the hydrolysis of the chloride, with the formation of 3-hydroxy-3-phosphonoisobenzofuranone (**6**) (see Scheme 2).

In addition, it was shown that refluxing an aqueous solution of **5** could also lead to **6**. The structural assignments of isobenzofuranones **5** and **6** are based on elemental analysis as well as ¹H, ³¹P and ¹³C NMR spectroscopic results. In addition to the ³¹P signals of **5** and **6** which are consistent with those of α -hydroxyphosphonates, also the ¹³C signals at 106 and 107 ppm ($J_{PC} \sim 200$ Hz) obtained for the benzylic carbons of **5** and **6** confirm these structures. Carbonyl carbons of acylphosphonates show signals at around 200 ppm also with J_{PC} coupling constants of ~ 200 Hz.

§ Following our conference presentation, there were two reports²⁷ on the formation of compound **6** and its silyl derivatives *via* silylation of phthalic anhydride.



Ring-chain tautomerism of phosphonoisobenzofuranone derivatives

Subsequently, the pH dependence of the NMR spectra of compounds **5** and **6** was studied. Addition of base to D₂O solutions of **5** and **6** caused marked changes, especially in the ³¹P and ¹³C NMR spectra. In compound **5**, changing the pH from 1 to 10 caused the ³¹P peak to shift from 10 to 0.89 ppm, while in the ¹³C spectrum the signal at 106 ppm ($d, J_{PC} = 199$ Hz), assigned to the benzylic carbon, was replaced by a new resonance for the carbonyl carbon at 216 ppm ($d, J = 179$ Hz). These changes are consistent with the opening of the heterocyclic ring in **5**, leading to the *ortho*-(phosphonoformyl)benzoate derivative, **7** (see Scheme 2). This assignment is supported by the very low field position and the large one-bond P–C coupling constant of the new signal in the ¹³C spectrum, and the new signal in the ³¹P spectrum, both characteristic of the acylphosphonate structure **7**. Similarly, the spectrum of **6** has changed upon raising the pH of the aqueous solution. The ³¹P signal was shifted from 8.9 to 0.19 ppm as expected for an acylphosphonate phosphorus atom, while the ¹³C signal for the carbonyl carbon appeared at 221 ppm

(d, $J = 160$ Hz), again consistent with the *ortho*-(phosphonato-formyl)benzoate structure **8** (see Scheme 2).¹²

Furthermore, it was found that acidification of *ortho*-(phosphonoformyl)benzoic acid derivatives **9** and **10** caused their rapid cyclization to **5** and **6**, respectively (see Scheme 2).

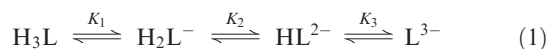
This ready cyclization is a consequence of the high reactivity of the carbonyl groups in **9** and **10**, caused by the strong electron withdrawing effect of the phosphonic group.¹³ There is a general consensus regarding the stabilizing influence of electron withdrawing groups on the cyclic tautomers of oxocarboxylic acid derivatives.^{14,15}

Advanced NMR and analytical studies

Following this stage of our synthetic and structural investigations carried out in Jerusalem, the Düsseldorf group decided to look deeper into this interesting combination of ring-chain tautomerism and protolytic equilibria. This was done using suitable hard- and software tools for the determination of macroscopic and microscopic dissociation constants *via* NMR controlled titrations,¹⁶ as described below.

The macroscopic model

In a starting phase a hypothetical macroscopic description of dissociation equilibria has been used following the conventional notation:



Acid dissociation constants $\text{p}K_1$ – $\text{p}K_3$ have been determined by high precision potentiometric titration of the title compound **6** with tetramethylammonium hydroxide (TMAOH) using the MINI-T setup,¹⁷ followed by iterative refinement of the titration curve (see Fig. S1 in ESI†) by WINSORE,¹⁸ two program systems developed in our laboratories. The resulting dissociation constants are listed in Table 1, including also those from the evaluation of the NMR-controlled titration (see below).

The molar fraction diagrams $\chi_i = f(\text{pH})$ and $\chi_i = f(\tau)$ shown in Fig. 1 and 2 clearly indicate the successive deprotonation to a trianion. For clearness sake we use the conventional reduced parameter τ to characterize the state of deprotonation where τ is defined as the ratio $\tau = n(\text{moles of TMAOH})/n(\text{moles of H}_3\text{L})$.

The parent benzoylphosphonic acid was characterized by $\text{p}K_1 = 0.39$ and $\text{p}K_2 = 5.60$ ²⁰ while for benzoic acid $\text{p}K = 4.20$ ²¹ was found. Early investigations on *ortho*-formyl-, acetyl- and benzoyl-substituted benzoic acids in equilibrium with

Table 1 The macroscopic dissociation constants for 3-hydroxy-3-phosphonoisobenzofuranone (**6**) as derived from WINSORE¹⁸ evaluation of potentiometric data (method A) and OPIUM¹⁹ evaluation of the NMR-controlled titration (method N) (simultaneous fit on the potentiometric, one ³¹P NMR and five ¹H NMR datasets; see below)

Method	A	B	A
Titration	1 M TMAOH	1 M TMAOH	0.1 M TMAOH
$\text{p}K_1$	0.65 ± 0.14	0.445 ± 0.008	1.15 ± 0.05
$\text{p}K_2$	5.90 ± 0.11	5.792 ± 0.003	5.88 ± 0.01
$\text{p}K_3$	6.57 ± 0.06	6.486 ± 0.002	6.75 ± 0.01

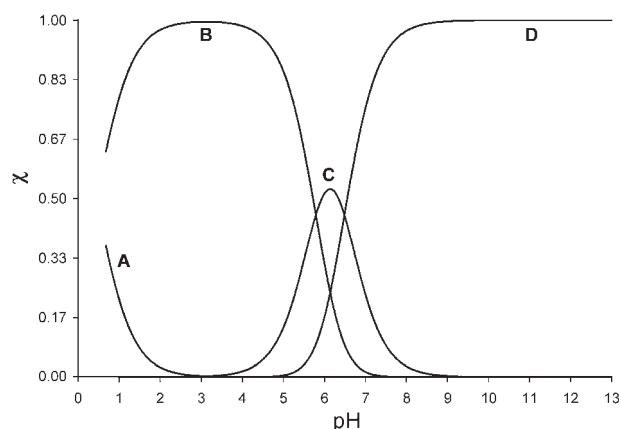


Fig. 1 Molar fraction diagram $\chi_i = f(\text{pH})$ for macroscopic protolytic species derived from **6**. Traces: (A) H_3L , (B) H_2L^- , (C) HL^{2-} , (D) L^{3-} .

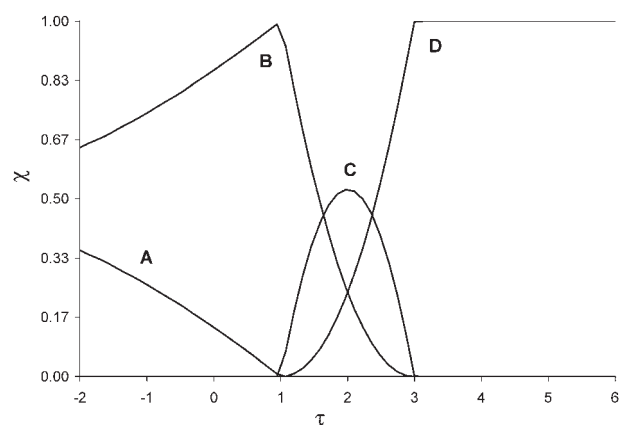


Fig. 2 Molar fraction diagram $\chi_i = f(\tau)$ for macroscopic protolytic species derived from **6**. Traces: (A) H_3L , (B) H_2L^- , (C) HL^{2-} , (D) L^{3-} .

corresponding ring-forms yielded $\text{p}K$ values of 4.56, 4.14²² and 3.53,²³ respectively. Hence, it is tempting to assign the three $\text{p}K$ values found for the title compound **6** to three elementary steps:

- $\text{PO}_3\text{H}_2 \rightarrow \text{PO}_3\text{H}^-$,
- $\text{COOH} \rightarrow \text{COO}^-$,
- $\text{PO}_3\text{H}^- \rightarrow \text{PO}_3^{2-}$

In order to identify the structures of species involved in simultaneous ring-chain and protolytic equilibria, multi-nuclear NMR techniques were applied:

202-MHz ³¹P{¹H} NMR controlled titrations

Results from 202-MHz ³¹P{¹H} NMR controlled titrations were obtained as the characteristic correlations of chemical shifts *vs.* τ or pH respectively, *e.g.* Fig. 3 shows the τ - δ stacked plot. (Corresponding pH- δ stacked, and the contour plots of τ - δ and pH- δ correlations are shown in ESI† as Fig. S2 to S4).

Fig. 3 is a pseudo-2D NMR spectrum, where the *x*-axis represents (as usual) the chemical shift, while the *y*-axis shows

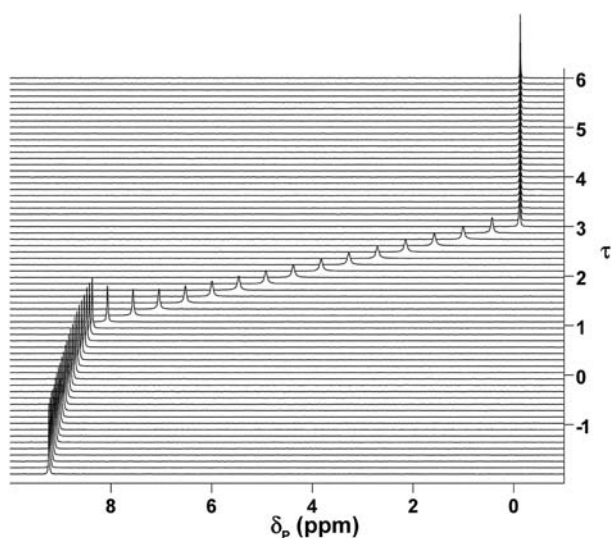


Fig. 3 202-MHz $^{31}\text{P}\{^1\text{H}\}$ NMR controlled titration of **6** with 1 M TMAOH. Stacked τ - δ plot: chemical shift δ_P (ppm) correlated with degree of titration τ .

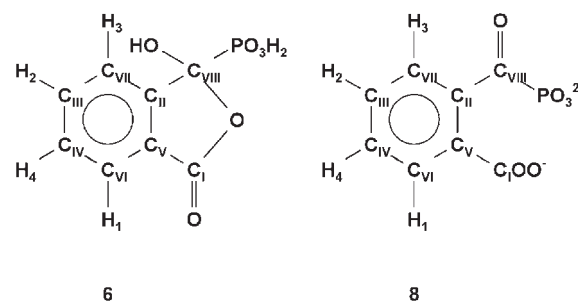
an analytical parameter, here the degree of titration τ . For more explanations of NMR-controlled titrations, see ref. 17.

It is evident from Fig. 3, that the first deprotonation step $\text{PO}_3\text{H}_2 \rightarrow \text{PO}_3\text{H}^-$ (associated with a $\text{p}K < 1$) is terminated at $\tau = 1$. The next two steps are more difficult to understand. A characteristic upfield shift corresponding to the deprotonation of $\text{PO}_3\text{H}^- \rightarrow \text{PO}_3^{2-}$ is observed but it is spanning over a titration range of 2τ values instead of one. In addition only one minimum is found for the first derivative $d\delta_P/d\text{pH}$, near pH 6 (see Fig. S5 in ESI†).

These findings indicate a simultaneous deprotonation for $\text{PO}_3\text{H}^- \rightarrow \text{PO}_3^{2-}$ and $\text{COOH} \rightarrow \text{COO}^-$. In addition, it is interesting to note the maximum in spectral half-width HW at $\tau = 2$ (see Fig. S6 in ESI†), which might be indicative for hydrogen bridges within or between the protolytic species, or with other slow exchange reactions as will be mentioned below.

Neglecting the inherent problems of microscopic dissociation at this stage, the macroscopic ion specific ^{31}P chemical shifts of species H_iL and corresponding deprotonation gradients $\Delta_P = \delta_P(\text{H}_{i-1}\text{L}) - \delta_P(\text{H}_i\text{L})$ are listed in Table 2.

The fully deprotonated species exhibits a chemical shift δ_P of -0.127 ppm which is consistent with data for the parent benzoylphosphonate anion moiety $\delta_P(\text{C}_6\text{H}_5\text{COPO}_3^{2-}) = -0.024$ ppm.²⁰ Henceforth the notation “**6–8**” will symbolize



Scheme 3

the genuine equilibrium mixture of protolytic species **6** and **8** (see Schemes 2 or 3 and the discussion below).

500-MHz ^1H NMR-controlled titrations

In order to prepare for the ^1H NMR-controlled titrations, high-resolution 500 MHz ^1H NMR spectra of **6** were recorded in D_2O and $\text{KOD-D}_2\text{O}$ solutions, followed by spectral analysis and iteration of the resulting ABCDX spin systems. Individual protons were assigned by means of 1D NMR (^1H , $^1\text{H}\{^{31}\text{P}\}$, $^{13}\text{C}\{^1\text{H}\}$) and 2D NMR (H_iH -COSY, H_iC -COSY, HMBC) methods.²⁴ A problem-specific spin enumeration was used in Scheme 3 and in Table 3: four aromatic protons H_1 – H_4 and eight carbon atoms C_1 – C_{VIII} ordered monotonously with decreasing frequencies as observed for a solution of 3-hydroxy-3-phosphonoisobenzofuranone, **6–8**, in D_2O .

The occurrence of significant changes of chemical shifts—shown in Table 3—indicate ring-opening and a total deprotonation to the *ortho*-phosphonatoformylbenzoate trianion. Characteristic deprotonation gradients $\Delta = \delta(\text{in KOD}) - \delta(\text{in D}_2\text{O})$, which indicate those structural changes, are listed in Table S1 (ESI†).

After having assigned unequivocally the four aromatic protons H_1 – H_4 , the HR 500 MHz ^1H NMR spectra shown in Fig. 4, were analyzed and iterated using WINDAISY.²⁵ (For corresponding numerical results from iterations see Table S2 in ESI†).

More detailed information about the ring-chain and protolytic equilibria have been derived from a 500 MHz ^1H NMR-controlled titration, as shown in the characteristic stacked τ - δ -plot of Fig. 5. (For τ - δ - and pH - δ -plots in contour and stacked representations see Fig. S7–S9 in ESI†).

Macroscopic constants from simultaneous iteration of ^1H and $^{31}\text{P}\{^1\text{H}\}$ NMR titration data

The OPIUM program¹⁹ enabled the simultaneous evaluation of the potentiometric and five NMR (4 H and 1 P) titration datasets of **6** at $I = 1$ M (TMACl), yielding the ion-specific chemical shifts listed in Table 4 along with the $\text{p}K$ values shown in Table 1.

The excellent fit of data can be visualized by δ_P -pH and δ_{H} -pH plots (see Fig. S10 and S11; the fitted potentiometric titration curve is shown in Fig. S12, see ESI†).

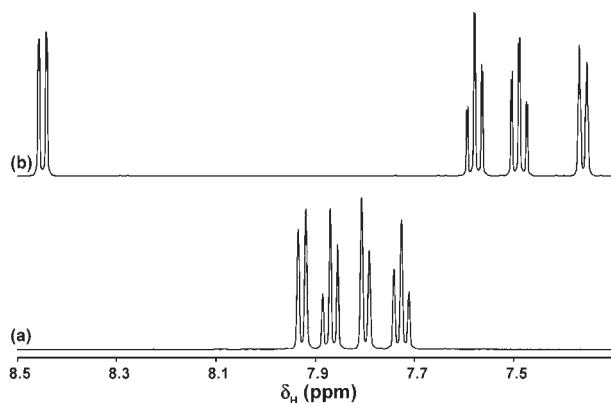
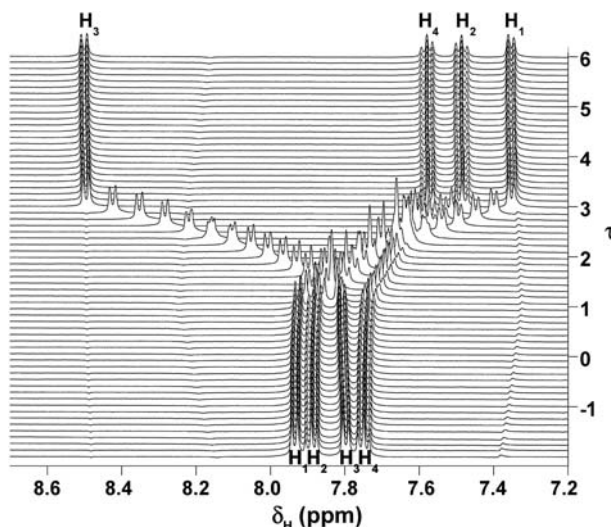
From Table 4 and Fig. 5, S10, S11 it follows that peak positions of all the four protons H_1 – H_4 are sensitive to $\text{p}K_2$ and $\text{p}K_3$. In addition, H_3 and H_4 are weak indicators for $\text{p}K_1$.

Table 2 Macroscopic ion specific parameters for δ_P (ppm) and deprotonation gradients Δ_P (ppm) of **6–8**

Species, H_iL	Chemical shift, δ_P	Gradient, Δ_P
H_3L	10.277 ± 0.007	
H_2L^-	8.371 ± 0.003	-1.906 ± 0.008
HL^{2-}	4.292 ± 0.005	-4.079 ± 0.006
L^{3-}	-0.127 ± 0.001	-4.419 ± 0.005

Table 3 Correlations from H_2C -COSY, 1H and $^{13}C\{^1H\}$ NMR studies of **6–8**. For enumeration of spins see Scheme 3. Chemical shifts δ_H (ppm) and δ_C (ppm)

D ₂ O (0.2510 M)				1 M KOD (0.1919 M)			
	δ_H		δ_C		δ_H		δ_C
H ₁	7.9262	C _{VI}	128.229	H ₁	7.3534	C _{VI}	129.123
H ₂	7.8693	C _{III}	138.289	H ₂	7.4826	C _{III}	130.376
H ₃	7.7980	C _{VII}	126.622	H ₃	8.4427	C _{VII}	134.171
H ₄	7.7258	C _{IV}	133.998	H ₄	7.5729	C _{IV}	135.013
		C _I	174.044			C _I	181.811
		C _{II}	148.941			C _{II}	142.240
		C _V	128.397			C _V	137.456
		C _{VIII}	107.439			C _{VIII}	219.432

**Fig. 4** 500-MHz 1H NMR spectrum of 3-hydroxy-3-phosphonoisobenzofuranone (**6–8**), (a) in KOD; (b) in D₂O.**Fig. 5** 500 MHz 1H NMR-controlled titration of **6** with 1 M TMAOH. Stacked τ - δ -plot. Chemical shift δ_P (ppm) correlated with degree of titration τ .

H₁ and H₃ are located closer than H₂ and H₄ to the furanone ring and the protolytic centers, and consequently show the strongest, but opposite effects, in chemical shifts. The first deprotonation takes place accordingly at PO₃H₂ → PO₃H[−], leaving the isobenzofuranone ring intact. The following two deprotonation steps are accompanied by ring-chain-opening. Further analysis of the ^{31}P and 1H NMR titration curves

Table 4 Macroscopic ion specific chemical shifts δ_H (ppm) and δ_P (ppm) for protolytic species derived from **6**. Error estimates: 0.002 ppm for δ_H and 0.02 ppm for δ_P

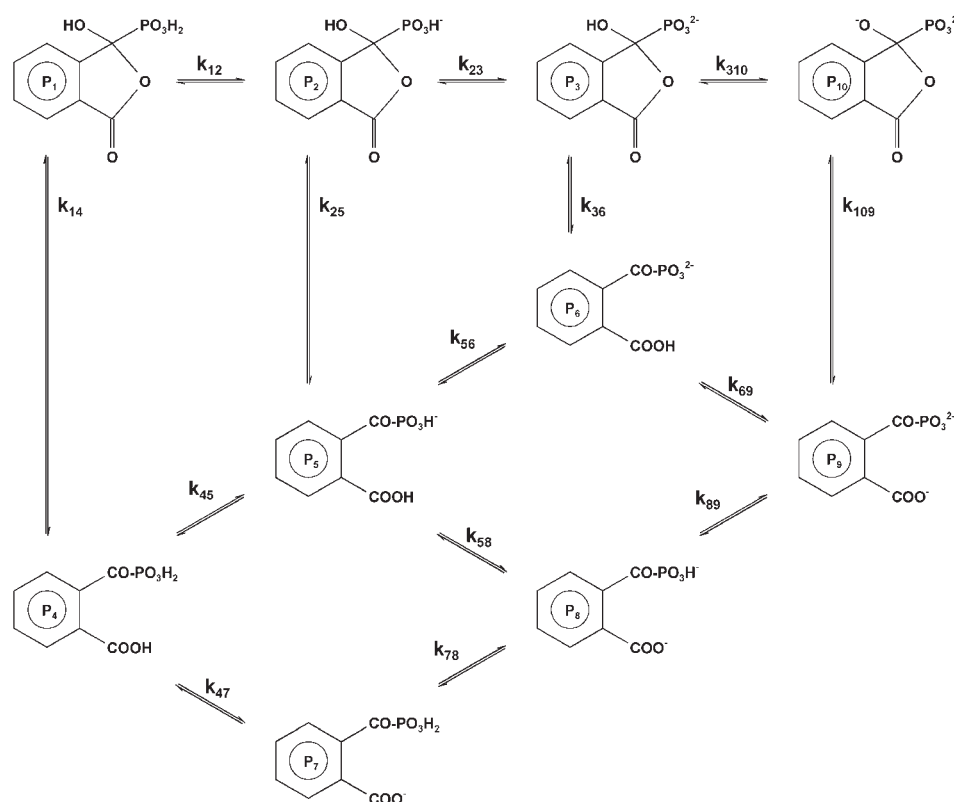
Species, H _i L	Specific chemical shift, δ				
	H ₁	H ₂	H ₃	H ₄	P
L	7.353	7.486	8.499	7.578	−0.13
HL	7.744	7.712	7.893	7.658	4.35
H ₂ L	7.926	7.882	7.810	7.740	8.38
H ₃ L	7.951	7.902	7.777	7.769	10.80

suggests that the numerical values of the site-specific dissociation constants of the phosphonic and carboxylic groups must be very close to each other, giving rise to a simultaneous microscopic dissociation of both functions.

The complex situation of concerted ring-chain tautomerism and protolytic equilibria

Evidence given above has established that the isobenzofuranone skeleton is stable below and up to pH 4 ($\tau = 1$), while the *ortho*-phosphonatoformylbenzoate skeleton is dominant at and above pH 10 ($\tau = 3$). In order to facilitate the understanding of the complex nature of the concerted equilibria, the apparent macroscopic protolytic processes and the microscopic and submicroscopic steps have been combined in Scheme 4. For clarity the microscopic species were enumerated systematically as shown in Scheme 4.

Equilibria indicated by vertical arrows ($\uparrow \downarrow$ k_{14} , k_{25} , k_{36} , k_{109}) involve ring-chain tautomerism, while the other equilibria refer to protonation/deprotonation of POH ($\leftarrow \rightarrow$ k_{12} , k_{23} ; \rightleftharpoons k_{45} , k_{56} , k_{78} , k_{89}), COOH (\rightleftharpoons k_{47} , k_{58} , k_{69}) and COH ($\leftarrow \rightarrow$ k_{310}) functions. In fact, a total of 14 elementary constants form a redundant set, since they are connected by Hessian constraints²⁶ characteristic to thermodynamic cycles. Since each cycle decreases the number of degrees of freedom by one²⁶ and there are seven such cycles in the system, 9 independent equilibrium constants are sufficient for the full description of the interconversion of ten distinct chemical entities. At the current stage of analysis, only the three macroscopic constants are known, thus the system is highly underdetermined and cannot be fully resolved without *a priori* simplifying assumptions. The 1H NMR chemical shift changes presented in the previous section suggest that species P₄ and P₆



Scheme 4

in Scheme 4 are less favored and the main routes of deprotonation might follow three alternative routes:

- (a) $P_1 \rightarrow P_2 \rightarrow P_3 \rightarrow P_6 \rightarrow P_9$
- (b) $P_1 \rightarrow P_2 \rightarrow P_5 \rightarrow P_8 \rightarrow P_9$
- (c) $P_1 \rightarrow P_2 \rightarrow P_5 \rightarrow (P_6, P_8) \rightarrow P_9$

Some arguments in favor of route (c) were derived from $^{13}\text{C}\{^1\text{H}\}$ NMR studies as described in the next section.

$^{13}\text{C}\{^1\text{H}\}$ NMR studies

Further evidence for this set of concerted equilibria of **6** were derived from 125 MHz $^{13}\text{C}\{^1\text{H}\}$ NMR spectra, shown in Fig. 6, obtained at six selected titration states ($0 \leq \tau \leq 3$). (Explicit data for chemical shifts δ_{C} are listed in Table S3 in ESI†). Table 5 lists the characteristic τ -step gradients $\Delta_{ij} = \delta(\tau = i) - \delta(\tau = j)$ indicating the chemical shift changes induced by addition of one equivalent base.

Arguments in favor of deprotonation route (c). The resonance lines of C_1 and C_{VIII} are very sensitive to τ . C_1 in COO lactone is visible only for τ from 0 to 1. The C_1 in the COO^- anion at $\tau = 3$ and C_{VIII} in the keto group at $\tau = 3$ exhibit characteristic chemical shifts. C_{VIII} in the COH group in the ring is visible only for τ from 0 to 1. C_{II} and C_{V} are strongly dependent on τ supporting the existence of the ring form for τ from 0 to 1. C_{III} and C_{VII} are less sensitive than C_1 and C_{VIII} but also support the ring structure for τ from 0 to 1. C_{VI} and C_{IV} are less sensitive than C_{III} and C_{VII} to changes in τ but still follow the tendencies

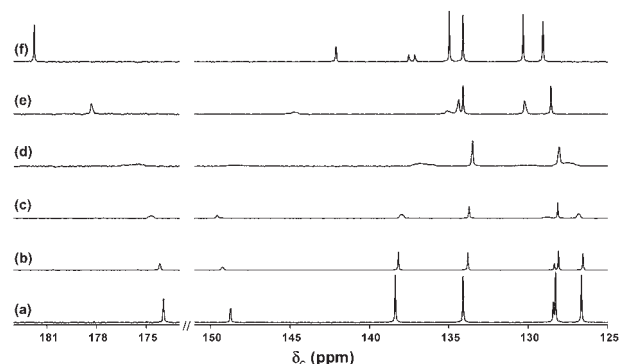


Fig. 6 $^{13}\text{C}\{^1\text{H}\}$ NMR spectra monitored for six selected titration states of species **6–8**, from bottom to top ((a)–(f)): $\tau = 0; 0.5; 1; 1.5; 2; 3$ for two regions (left) $\text{COOH}/\text{COO}^- \text{C}_1$; (right) $\text{C}_{\text{II}}\text{--}\text{C}_{\text{VII}}$.

shown above. The deduced structural features of the dominant protolytic species of **6** are summarized in Table 6. Finally, ^1H and $^{13}\text{C}\{^1\text{H}\}$ NMR spectra of (a) phthalaldehydic acid, (b)

Table 5 τ -Step gradients (ppm) $\Delta_{ij} = \delta_{\text{C}}(\tau = i) - \delta_{\text{C}}(\tau = j)$, differences of ion-specific δ_{C} chemical shifts of **6**

	Δ_{10}	Δ_{21}	Δ_{32}	Δ_{31}
C_1	+0.71	+3.63	+3.57	+7.20
C_{II}	+0.82	−4.77	−2.59	−7.36
C_{III}	−0.41	−3.62	−3.90	+7.52
C_{IV}	−0.40	+0.38	+0.99	+1.37
C_{V}	+0.41	+6.23	+2.39	+8.62
C_{VI}	−0.16	+0.43	+0.64	+1.07
C_{VII}	+0.14	+3.43	+3.99	+7.42

Table 6 Arguments in favor of deprotonation route (c) in compound 6. For structures of species involved in exchange reactions (P_1 , P_2 , P_6 , P_8 , P_9) see Scheme 4

τ	Species	Proposed structure
0.0	Mixture of P_1 and P_2	Ring, stationary
0.5	Mixture of P_1 and P_2	Ring
1.0	P_2	Ring
1.5	Mixture of P_2 , P_6 , P_8 , P_9^-	Ring, and chain in exchange
2.0	Mixture of P_2 , P_6 , P_8 , P_9	Ring, and chain in exchange No evidence for P_3 ring
3.0	P_9	Chain, stationary

phthalide, and (c) compound 5 were compared with those of 6, also supporting the ring nature of dissociation species P_1 and P_2 bearing substituents $-\text{PO}_3\text{H}_2$ and $-\text{PO}_3\text{H}^-$, respectively.

At the present stage of our knowledge and information accessible in the open literature, it is impossible to determine the full set of microscopic dissociation constants. But with respect to the Hessian nature, apparent macroscopic and microscopic constants are connected for routes (a) and (b) by eqn (2) and for route (c) by eqn (3), where k_{25} and k_{36} represent the ring-to-chain tautomerism constants.

$$K_2K_3 = k_{23}k_{36}k_{69} = k_{25}k_{58}k_{89} \quad (2)$$

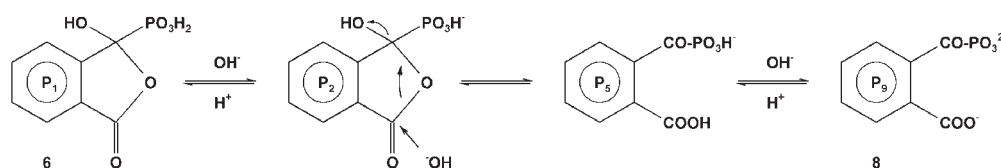
$$K_2K_3 = k_{25}k_{57}k_{79} = k_{25}k_{58}k_{89} \quad (3)$$

It is interesting to note the significant line broadening effects within the range $1 < \tau < 2$ indicating slow exchange processes. Dynamic NMR was used previously to elucidate the ring-chain kinetics in the pair of 3-hydroxy-3-(methyl- d_3)isobenzofuranone and 3-(acetyl- d_3)benzoic acid,¹⁰ⁿ respectively.

Conclusion

Our multinuclear NMR titration results reveal that the state of ionization of the phosphonic group governs the position of the ring-chain tautomeric equilibrium between species 6 and 8. The ring opening does not take place until the first ionization of 6 is completed, or conversely, the fully ionized *ortho*-phosphonato-formylbenzoate (8) does not undergo cyclization (see Scheme 5). It is reasonable to assume this reduced tendency of 8 to cyclize is the consequence of the reduced electrophilicity of the keto group, caused by the diminished electron withdrawing effect of the doubly ionized phosphonate group.

The ring-chain tautomerism constants involved in Scheme 4 are not accessible *via* the NMR methods presented here. Complementary IR or UV spectroscopic approaches might help in the future to resolve the full equilibrium system. The problem presented in this paper is considerably more complex than those of the parent 3-hydroxyisobenzofuranones studied previously.¹⁰



Scheme 5

Experimental

(a) Syntheses

3-Chloro-3-(dimethylphosphono)isobenzofuranone (3) was prepared according to a known procedure.¹¹

Sodium 3-chloro-3-(methylphosphonato)isobenzofuranone (4). Compound 3 (8.87 g, 0.032 mol) and NaI (5.06 g, 0.033 mol) were dissolved in dry MeCN (100 mL) and left to stand at room temperature for 2 days. The white precipitate was filtered off and washed with dry MeCN (4×15 mL) and dried *in vacuo*. An additional amount of product was obtained by evaporating the mother-liquor. Yield: 8.7 g (95%), mp 180–185 °C (decomp.). NMR (D_2O): ^{31}P : 7.0 (q, $J = 10.4$ Hz); ^1H : 7.65 (m, 3 H, arom), 7.45 (m, 1 H, arom), 3.49 (d, 3 H, $J = 10.2$ Hz, CH_3OP); ^{13}C : 171, 149, 137, 133, 126, 125, 124, 95 (d, $J_{\text{PC}} = 177$ Hz, CCIP), 56 (d, $J_{\text{POC}} = 6.8$ Hz, POCH_3). Anal. Calc. for $\text{C}_9\text{H}_7\text{ClO}_5\text{PNa}$, C, 37.99, H, 2.48, Cl, 12.46. Found: C, 37.68, H, 2.63, Cl, 12.11%.

3-Hydroxy-3-(methylphosphono)isobenzofuranone (5). A solution of compound 4 (2 g, 0.07 mol) in distilled water (20 mL) was kept at room temperature for 4 days. The solution was evaporated *in vacuo*, and then co-evaporated with MeCN (2×30 mL) to a syrup, which was taken up in MeCN (50 mL), to separate NaCl which was filtered off, and the organic filtrate evaporated *in vacuo* to a white solid residue. An analytical sample was obtained by recrystallization from MeCN–diethyl ether. Yield: 1.6 g (94%). mp 208–209 °C. NMR (D_2O): ^{31}P , 10.2 ppm (q, $J_{\text{POCH}} = 9.7$ Hz); ^1H : 7.5 (m, 4 H, arom), 3.40 (d, 3 H, $J_{\text{POCH}} = 10.2$ Hz, POCH_3); ^{13}C : 173, 148, 137, 133, 127, 126, 125, 106 (d, $J_{\text{PC}} = 199$ Hz, CP), 55 (d, $J_{\text{POC}} = 7.1$ Hz, POCH_3). MS: 226 ($\text{M} - \text{H}_2\text{O}$). Anal. Calc. for $\text{C}_9\text{H}_9\text{O}_6\text{P}$: C, 44.28; H, 3.72. Found: C, 43.99, H, 3.65%.

3-Hydroxy-3-phosphonoisobenzofuranone (6)

(a) *From 4.* A solution of compound 4 (2 g, 0.007 mol) in distilled water (50 mL) was refluxed for 2.5 h. The solution was evaporated then co-evaporated with MeCN (2×30 mL) to a syrup, which was taken up in MeCN (50 mL) to remove the NaCl by filtration. Evaporation of the organic phase *in vacuo* gave a white foam which was recrystallized from water–MeCN. Yield: 1.35 g (90%), mp 196–198 °C. NMR (D_2O): ^{31}P 8.96 (s); ^1H : 7.4 (m); ^{13}C : 172 (d, $J = 4.5$ Hz), 147 (d, $J = 5.3$ Hz), 137, 132, 127, 126, 125, 107 (d, $J_{\text{PC}} = 198$ Hz). MS: 148 ($\text{M} - \text{H}_3\text{PO}_3$). Anal. Calc. for $\text{C}_8\text{H}_7\text{O}_6\text{P} \cdot 0.25\text{H}_2\text{O}$: C, 40.98; H, 3.20. Found: C, 40.78; H, 3.11%.

(b) *From 5.* A solution of compound 5 (0.02 g) in D_2O (0.4 mL) was refluxed for 2.5 h. 5 was converted to the extent of 95% to 6 and MeOH as shown by NMR (^{31}P and ^1H). NMR ^{31}P (D_2O): 8.96 (s). ^1H : 7.4 (m, 4H, arom); and 3.17 (s, 3H, MeOH).

Disodium *ortho*-(methylphosphonato)formylbenzoate (7). To a solution of compound **5** (60 mg) dissolved in D₂O (0.4 mL) solid Na₂CO₃ was added until pH 10. Examination of the solution by NMR spectroscopy gave the following results: ³¹P: 0.89 (q, *J* = 9.3 Hz). ¹H: 7.6 (m, 4H, arom), 3.45 (d, *J* = 10.2 Hz, 3H, POCH₃). ¹³C: 216 (d, *J*_{PC} = 179 Hz), 181, 166, 142, 141 (d, *J* = 50 Hz), 137, 135, 133, 132, 57 (d, *J* = 6 Hz). The solution was evaporated to a syrup which was dried *in vacuo*.

Trisodium *ortho*-phosphonatoformylbenzoate (8). Compound **6** (63 mg) was dissolved in D₂O (0.4 mL). Na₂CO₃ was added until pH 10. Examination of the solution by NMR spectroscopy gave the following results: ³¹P: −0.19 (s). ¹H: 7.6 (m, arom); ¹³C: 221 (d, *J* = 160 Hz), 183, 168, 144 (d, *J* = 1.4 Hz), 139 (d, *J* = 47 Hz), 137, 136, 133, 131. The solution was evaporated *in vacuo* to a syrup which was dried *in vacuo* over P₄O₁₀.

(b) Analytical and NMR studies

In order to determine the dissociation constants, three potentiometric titrations with 0.1 M and 1.0 M TMAOH were performed under nitrogen atmosphere. Apparatus and software: MINI_T.¹⁷ Titration data were iterated with WINSCORE.¹⁸

Titration with 0.1 M TMAOH: 25 ml of a solution containing 0.18 mmol of 3-hydroxy-3-phosphonoisobenzofuranone (**6**), 0.36 mmol of HCl and 2.5 mmol of TMACl was titrated with 0.1010 M TMAOH at 25 ± 0.1 °C.

Titration with 1.0 M TMAOH: 25 ml of a solution containing 1.75 mmol of 3-hydroxy-3-phosphonoisobenzofuranone (**6**), 2.50 mmol of HCl and 25 mmol of TMACl was titrated with 1.0220 M TMAOH at 25 ± 0.1 °C.

NMR spectrometer: Bruker AVANCE DRX 500 equipped with a 5 mm QNP ¹H/¹³C/³¹P/¹⁹F Z-grad probe or 5 mm TBI probe. Pulse programs: ¹H NMR zg30; ¹³C{¹H} and ³¹P{¹H} NMR zgpg30.

Spectral parameters for Fig. 4: Trace (a): 43.3 mg of **6** in 0.75 ml D₂O. Int. ref.: (CH₃)₃SiCH₂CH₂CH₂SO₃Na. Trace (b): 33.1 mg of **6** in 0.75 ml of 1 M KOH in D₂O. Int. ref.: (CH₃)₃SiCH₂CH₂CH₂SO₃Na. ¹H NMR (Bruker notation in parentheses): Size of FID (TD): 65 536. Number of scans (NS): 128. Spectral width (SWH): 5482 Hz. Acquisition time (AQ): 5.98 s. Pre-scan delay (DE): 6 μs. Transmitter frequency (SFO1): 500.1322506 MHz. Size of real spectrum (SI): 32768 Hz. Spectral resolution (HzpPT): 0.1673 Hz. Window function (WDW): EM. Line broadening (LB): 0.30.

Spectral parameters for Fig. 6, Table 3 and Table S3: Standard solution: 57.85 mg of **6** in 0.50 ml D₂O. Int. ref.: (CH₃)₃SiCH₂CH₂CH₂SO₃Na. Addition of 1 M NaOH in D₂O to adjust degree of titration τ: (a) 0 ml, τ = 0; (b) 0.125 ml, τ = 0.5; (c) 0.25 ml, τ = 1; (d) 0.375 ml, τ = 1.5; (e) 0.5 ml, τ = 2; (f) 0.625 ml, τ = 2.5; (f) 0.75 ml, τ = 3. ¹³C{¹H} NMR. TD: 65 536. NS: 1024. SWH: 32 680 Hz. AQ: 1 s. DE: 6 μs. SFO1: 125.772201 MHz. SFO2: 500.1320006 MHz. SI: 131072 Hz. HzpPT: 0.2493 Hz. WDW: EM. LB: 5.

Software packages used for spectral evaluation: Bruker Win-NMR 6.2 and Bruker XWIN-NMR 2.6 (Comments to Fig. 3, 5, S2–S4, S7–S9: We pioneered the technology of

(almost fully) automated NMR titration and described details of NMR, analytics, hardware, software, corresponding mathematical background in papers and reviews listed under ref. 16).

The setup for NMR-controlled titration of **6**: 445.7 mg (1.918 mmol) of **6**, 3.847 mmol of HCl, and 2.5 mmol of TMACl were dissolved in H₂O to make up a total volume of 25 ml. This sample solution was titrated with a 0.9840 M TMAOH solution in H₂O to adjust the degree of titration τ in 64 steps within the range from τ = −2 to τ = 6. Spectral parameters: ¹H NMR: TD: 32 768. NS: 128. SWH: 5296 Hz. AQ: 5.98 s. DE: 6 μs. SFO1: 500.1322506 MHz. SI: 32 768 Hz. HzpPT: 0.1616 Hz. WDW: EM. LB: 0.30. ³¹P{¹H} NMR: TD: 16 384. NS: 16. SWH: 10163 Hz. AQ: 5.98 s. DE: 6 μs. SFO1: 202.4550727 MHz. SFO2: 500.1320005 MHz. SI: 16 384 Hz. HzpPT: 0.6202 Hz. WDW: EM. LB: 0.30.

All NMR spectra were recorded on a Bruker AVANCE DRX 500 spectrometer using a TXO-HPLC probe. The magnet field was not locked during the NMR-controlled titration, but remained sufficiently stable[¶] throughout the 24 h of the NMR titration.¹⁶ Chemical shifts were referenced using external (CH₃)₃CH₂CH₂CH₂SO₃Na and 85% H₃PO₄.

Acknowledgements

E. B. is affiliated with the David R. Bloom Center for Pharmacy. E. B. and G. H. are indebted to German Israeli Foundation (GIF) for a Research Grant (I-316-186-05/93). J. K. thanks the Rabin Foundation in Denmark for a generous grant. Z. Sz. is grateful to Deutscher Akademischer Austauschdienst (DAAD) for a two-year PhD scholarship in Düsseldorf. Special thanks (from G. H.) are due to Dr T. Keller, Bruker BioSpin, for four decades of NMR support.

References

- (a) *Bisphosphonate on Bones*, ed. O. L. M. Bijvoet, H. A. Fleisch, R. E. Canfield and R. G. G. Russell, Elsevier, 1995; (b) H. Fleisch, *Bisphosphonates in Bone Disease. From the Laboratory to the Patient*, The Parthenon Publishing Group, New York, 3rd edn, 1997, pp. 145–150.
- (a) P. G. Koutsoukos and C. G. Kontoyannis, *J. Cryst. Growth*, 1984, **69**, 367–376; (b) J. A. Mikroyannidis, *Phosphorus Sulfur Relat. Elem.*, 1987, **32**, 113–118.
- G. R. Mundy, *Bone*, 1987, **8**, S9–S16.
- (a) R. P. Rubin, G. B. Weiss and J. W. Putney, Jr, *Calcium in Biological Systems*, Plenum Press, NY, 1985; (b) F. J. Schoen, H. Harasaki, K. M. Kim, H. C. Anderson and R. J. Levy, *J. Biomed. Mater. Res., Appl. Biomater.*, 1988, **22**(Suppl. S), 11–36.

[¶] The TPI-probe and a D₂O sample were used to lock and shim the magnetic field as usual. Subsequently the D₂O sample was replaced by a 0.162 M solution of 1-Hydroxy-ethane-1,1-diphosphonic acid (HEDP) in H₂O. The time dependence of the magnetic field strength for the Bruker AVANCE DRX 500 spectrometer under non-locked conditions was monitored for 24 h in intervals of 20 min for 202.46 MHz ³¹P{¹H} NMR. A variation in δ_P within a range of <0.01 ppm was observed, while the spectral resolution remained effectively constant. For a TXO-HPLC probe and a separate 0.00033 M solution of HEDP in D₂O a variation in δ_P of <0.018 ppm within 16 h was achieved. These results are definitely more than sufficient for practical evaluations of δ_P and demonstrate an excellent stability of the magnetic field strength and homogeneity.

- 5 (a) B. A. Bopp, C. B. Estep and D. Anderson, *J. Fed. Proc.*, 1977, **36**, 939; (b) S. M. Roberts, Design of Anti-viral agents other than nucleoside analogs, in *Antiviral Drug Development – A Multi-disciplinary Approach*, ed. E. De-Clercq and R. T. Walker, Plenum Press, New York, NY, 1988, pp. 37–54.
- 6 (a) G. Golomb, A. Schlossman, H. Saadeh, M. Levi, J. M. Van Gelder and E. Breuer, *Pharmacol. Res.*, 1992, **9**, 143–148; (b) J. M. Van Gelder, E. Breuer, A. Ornoy, A. Schlossman, N. Patlas and G. Golomb, *Bone*, 1995, **16**, 511–520; (c) D. Skrtic, N. Eidelman, G. Golomb, E. Breuer and E. D. Eanes, *Calcif. Tissue Int.*, 1996, **58**, 347–354.
- 7 R. Chen, A. Schlossman, E. Breuer, G. Hägele, C. Tillmann, J. M. van Gelder and G. Golomb, *Heteroat. Chem.*, 2000, **11**, 470–479.
- 8 M. Mathew, B. O. Fowler, E. Breuer, G. Golomb, I. S. Alferiev and N. Eidelman, *Inorg. Chem.*, 1998, **37**, 6485–6494.
- 9 K. D. Berlin, D. H. Burpo, R. U. Pagilagan and D. Bude, *Chem. Commun.*, 1967, 1060.
- 10 (a) D. D. Wheeler, D. C. Young and D. S. Erley, *Tetrahedron*, 1957, **22**, 547–556; (b) E. Bernatek, *Acta Chem. Scand.*, 1960, **14**, 785–788; (c) P. R. Jones, *Chem. Rev.*, 1963, **63**, 461–487; (d) P. R. Jones and P. J. Desio, *J. Org. Chem.*, 1965, **30**, 4293–4297; (e) M. S. Newman and C. Courduvelis, *J. Org. Chem.*, 1965, **50**, 1795–1800; (f) M. V. Bhatt and K. M. Kamath, *Tetrahedron Lett.*, 1966, **32**, 3885–3890; (g) J. Kagan, *J. Org. Chem.*, 1967, **32**, 4060–2250; (h) J. Finkelstein, T. Williams, V. Toome and S. Traiman, *J. Org. Chem.*, 1967, **32**, 3229–3230; (i) D. G. Buckley, E. Ritchie and W. C. Taylor, *Aust. J. Chem.*, 1969, **22**, 577–595; (j) R. P. Bell, B. G. Cox and B. A. Timimi, *J. Chem. Soc. B*, 1971, 2247–2250; (k) U. D. G. Prabhu, K. C. Eapen and C. Tamborski, *J. Org. Chem.*, 1984, **49**, 2792–2795; (l) K. Bowden and F. P. Malik, *J. Chem. Soc., Perkin Trans. 2*, 1993, 635–339; (m) W. M. Fabian and K. Bowden, *Eur. J. Org. Chem.*, 2001, 303–309; (n) L. Santos, A. Vargas, M. Moreno, B. R. Manzano, J. M. Luch and A. Douhai, *J. Phys. Chem. A*, 2004, **108**, 9331–9341; (o) K. Bowden and F. P. Maili, *J. Chem. Soc., Perkin Trans. 2*, 1993, 635–639.
- 11 For a detailed synthetic procedure, see: J. Kehler and E. Breuer, *Synthesis*, 1998, 1419–1420.
- 12 E. Breuer, in *The Chemistry of Organophosphorus Compounds*, ed. F. R. Hartley, John Wiley & Sons Ltd, Chichester, 1996, vol. 4, pp. 653–729.
- 13 J. Katzhendler, I. Ringel, R. Karaman, H. Zaher and E. Breuer, *J. Chem. Soc., Perkin Trans. 2*, 1997, 341–349; in this paper we report a σ^* value of 2.65 for the dimethoxyphosphinyl group, close to that of the trifluoromethyl group.
- 14 E.g. 2-trifluoroacetylbenzoic acid and 3-trifluoropropionic acid: C. Francese, M. Tordeux and C. Wakselman, *Tetrahedron Lett.*, 1988, **29**, 1029–1030.
- 15 The formation of cyclic products is characteristic of oxocarboxylic acids, especially *ortho*-acylbenzoic acids and related derivatives: R. E. Valters, F. Fülöp and D. Korbonits, *Adv. Heterocycl. Chem.*, 1995, **68**, 251–321, and references therein.
- 16 (a) G. Hägele, review "NMR Controlled Titrations of Phosphorus-Containing Acids and Bases in Protolysis and Complex Formation" in *Phosphorus-³¹P-NMR Spectral Properties in Compound Characterization and Structural Analysis*, ed. L. D. Quin and J. G. Verkade, VCH, Weinheim, 1994, pp. 395–409; (b) G. Hägele, Z. Szakács, J. Ollig, S. Hermens and C. Pfaff, *Heteroat. Chem.*, 2000, **11**, 562–582; (c) G. Hägele, M. Grzonka, J. Peters, H. Spiegl, H. W. Kropp, J. Ollig, S. Hermens, S. Augner, C. Uhlemann, C. Pfaff, Z. Szakács, T. Keller, M. Rindispacher and M. Spraul, *BRUKER NMR GUIDE2002*, Part of Software packages *TopSpin* and *XWIN-NMR* from Bruker BioSpin, Rheinstetten, Germany.
- 17 A. Bier, PhD Thesis, Heinrich-Heine-Universität Düsseldorf, 1993.
- 18 I. Reimann, PhD Thesis, Heinrich-Heine-Universität Düsseldorf, 2001.
- 19 M. Kyvala and I. Lukes, *International Conference, Chemometrics 95, Pardubice, Česká Republika*, University of Pardubice, Pardubice, 1995, p. 63, First presentation of the OPIUM program.
- 20 C. Arendt, PhD Thesis, Heinrich-Heine-Universität, Düsseldorf, 2002.
- 21 K. D. Bowden and G. R. Taylor, *J. Chem. Soc. B*, 1971, 1390–1394.
- 22 M. J. Tirouflet, *C. R. Hebd. Seances Acad. Sci.*, 1953, **236**, 1426.
- 23 L. G. Bray, J. F. J. Dippy and S. R. C. Hughes, *J. Chem. Soc.*, 1957, 265–267.
- 24 S. Augner, PhD Thesis, Heinrich-Heine-University, Düsseldorf, 2002.
- 25 (a) *WINDAISO*, A Novel Program System for Simulation and Iteration of High Resolution NMR Spectra, ed. U. Weber, R. Spiske, H.-W. Höfken, G. Hägele and H. Thiele, Manual and Program system, , *Bruker Manual*, 1993; (b) U. Weber and H. Thiele, *NMR Spectroscopy: Modern Spectral Analysis*, Wiley-VCH, Weinheim, 1998.
- 26 Z. Szakács and B. Noszál, *J. Math. Chem.*, 1999, **26**, 139–155.
- 27 (a) D. V. Griffiths and P. Duncanson, *Phosphorus, Sulfur Silicon Relat. Elem.*, 2002, **177**, 2213–2214; (b) E. Guenin, E. Degache, J. Liquier and M. Lecouvey, *Eur. J. Org. Chem.*, 2004, 2983–2987.